2.2. Synthesis of PIPAM-b-PBMA block copolymer

Hydroxyl-terminated poly(*N*-isopropylacrylamide) (PIPAM–OH) and carboxyl-terminated poly(butyl methacrylate) (PBMA–COOH) were prepared by telomerization using 2-mercaptoethanol (ME) and 3-mercaptopropionic acid as a chain transfer agent, respectively [15]. A molecular weight of the PIPAM–OH was determined by gel permeation chromatography (GPC; Tosoh, SC-8020, calibrated with polystyrene standards, elution rate: 1.0 ml/min) at 45 °C using DMF containing 10 mM LiCl as eluent. The terminal carboxyl functionality of the PBMA–COOH was determined by non-aqueous potentiometric titration using 0.01 N CH_3ONa dissolved in a mixture of methanol and dioxane. Diblock copolymers of PIPAM and PBMA (PIPAM-*b*-PBMA) were obtained by reaction between a hydroxyl group of the PIPAM–OH and a carboxyl group of the PBMA–COOH by activation with thionyl chloride. The detailed synthetic and purification procedures of the block copolymers were reported in our previous paper [15].

2.3. Synthesis of P(IPAM–co–DMAM)-b-PLA block copolymer

Hydroxyl-terminated thermoresponsive polymers, poly(IPAM–*co*–DMAM) (P(IPAM–DMAM)–OH) was synthesized by radical copolymerization (20 mol% DMAM against total monomers) using ME [17]. Diblock copolymers were synthesized by ring opening polymerization of D,L-lactide (LA) from the hydroxyl end-group of the P(IPAM–DMAM)–OH as reported in our previous paper [17]. Briefly, the P(IPAM–DMAM)–OH polymers were dissolved in xylene. D,L-lactide and tin(II)2-ethylhexanoate as a catalysis were added to the polymer solution. Polymerization proceeded at 150 °C for 24 h under a nitrogen atmosphere. The obtained polymers were precipitated twice in an excess of diethyl ether, and then dried in vacuo. A molecular weight of the P(IPAM–DMAM)-*b*-PLA block copolymers was determined by GPC in the same conditions as for the PIPAM-*b*-PBMA. The composition of the block copolymers was determined with a ^1H NMR spectrometer (400 MHz, Varian).

2.4. Preparation of DOX-loaded polymeric micelles

The formation of micelle structures and the DOX loading were simultaneously carried out by a dialysis method. The PIPAM-*b*-PBMA block copolymers (19 mg) and DOX–HCl (19 mg) were dissolved separately in 1.5 ml of *N*-ethylacetamide. The DOX solution was added to the polymer solution after addition of triethylamine (TEA) (6.0 μl, 1.3 molar equivalents versus DOX–HCl). The solution was dialyzed against distilled water at room temperature for 48 h (MWCO: 12,000–14,000, Spectra/Por 4, Spectrum Medical Industries). For the P(IPAM–DMAM)-*b*-PLA block copolymers, DOX–HCl (100 mg) was dissolved in 50 ml *N*,*N*-dimethylacetamide (DMAc) and added by TEA (1.5 molar equivalents versus DOX–HCl), followed by stirring for 10 min. P(IPAM–DMAM)-*b*-PLA block copolymers (100 mg) were dissolved in 50 ml DMAc. The DOX solution and the polymer solution were mixed at room temperature, followed by dialysis against distilled water using the dialysis membrane (MWCO: 12,000–14,000, Spectra/Por4) at room temperature. The obtained DOX-loaded polymeric micelles were ultrafiltrated using a filtration membrane of 200,000 molecular weight cut-off (ultrafilter Q2000, ADVANTEC MFS, INC.) at 4 °C to remove un-incorporated DOX. The UV absorbance at 485 nm was measured to estimate quantities of the incorporated DOX (V-530, Japan Spectroscopic Co., Japan) using molar extinction coefficient of DOX–HCl at 485 nm in distilled water.

2.5. Characterization of polymeric micelles

Optical transmittance of the 0.5 wt% polymeric micelle solutions (the PIPAM/PBMA micelles in water, and the P(IPAM–DMAM)/PLA micelles in phosphate buffer saline(PBS)) at various temperatures were measured at 600 nm with a UV–vis spectrometer. A sample cell was thermostated with a Peltier-effect cell holder (EHC-477, Japan Spectroscopic). Heating rate was 0.1 °C/min. The LCST of the micelle solutions was defined as the temperature inducing a 50% decrease in optical transmittance. Hydrodynamic diameters of the micelles were measured by dynamic light scattering (DLS) using a DLS-7000 instrument (Otsuka Electronics Co., Japan) equipped with He–Ne laser (633 nm).

2.6. Cell culture

Human breast cancer MCF-7 and its DOX-resistant (MCF-7/DOX) cell lines (kindly supplied by National Cancer Institute, USA) were grown as a monolayer in 75 cm^2 tissue culture flask containing

RPMI 1640 supplemented with 5% fetal bovine serum (FBS), 100 units/ml penicillin and 100 μg/ml streptomycin. All cell lines were cultured at 37 °C with 5% CO_2.

2.7. Intracellular distribution of DOX

Cells were plated at a density of 4×10^4 cells/well onto a glass slide with an aminoalkyl group-grafted surface (S-9215, Matsunami Glass, Japan) fitted with a culture vessel (flexiPERM, VIVASCIENCE, Germany). Cells were incubated in RPMI 1640 supplemented with 5% FBS, 100 units/ml penicillin and 100 μg/ml streptomycin. At 14 h after plating, cells were exposed to either free DOX (30 μg/ml) or the DOX-loaded micelles (incorporated DOX 30 μg/ml) in the cell culture medium and incubated at below (29 °C for the PIPAM/PBMA micelles, 37 °C for the P(IPAM–DMAM)/PLA micelles) or above (37 °C for the PIPAM/PBMA micelles, 42.5 °C or the P(IPAM–DMAM)/PLA micelles) the LCSTs of the micelles. After incubation for various periods, cells were gently rinsed with PBS to remove the micelles adhered to the cell membranes (non-incorporated micelles) at the temperature below the micelle LCST (25 °C). The cells on glass slides were fixed at room temperature with 4% paraformaldehyde for 30 min, and then washed with PBS containing 0.02% NaN_3. Nuclei of the treated cells were stained with Hoechst 33258 (10 μg/ml, Molecular Probes, USA) for 10 min at room temperature. Finally, the cells were washed three times with PBS containing 0.02% NaN_3 and observed by fluorescence microscopy (TE2000-U, Nikon, Japan) and laser scanning confocal microscopy (Leica TCS NT, Leica, Germany).

3. Results and discussion

3.1. Synthesis and characterization of the block copolymer

A molecular weight of the PIPAM-*b*-PBMA block copolymers were estimated from characterization of each polymer chain. Results are summarized in Table 1. For the P(IPAM–DMAM)-*b*-PLA block copolymers, molecular weights and polydispersities (PDI) were determined by GPC, and its molar ratios of IPAM, DMAM, and LA units were determined with a ^1H NMR spectrum using $CDCl_3$ as a solvent. Results are summarized in Table 2. Chemical structures of the block copolymers are shown in Fig. 1.

3.2. Characterization of polymeric micelles

Core-shell type micelle formation through self-association of the amphiphilic diblock copolymers and doxorubicin (DOX) loading were successfully achieved by dialysis of the polymer/drug mixtures in organic solvents against water at a temperature below the LCST of shell-forming polymer segments. For the PIPAM/PBMA micelles, a high DOX loading content (9.6 wt%) was obtained. The hydrodynamic diameters of the DOX-loaded PIPAM/PBMA micelles showed a relatively large distribution (338 nm, Fig. 2(a)). In general, particle size of mono-dispersed (not aggregated) polymeric micelle is known as 10–200 nm [5]. This larger particle size of the PIPAM/PBMA micelles was considered to be caused by the aggregation of individual polymeric micelles. On the other hand, a relatively low DOX incorporation (4.4 wt%) was obtained for the P(IPAM–DMAM)/PLA micelles. A possible explanation for a lower DOX content in the P(IPAM–DMAM)/PLA micelle is as the follows; (a) The PBMA inner cores possess higher hydrophobicity than the PLA cores due to hydrophobic butyl side chains, and (b) the crystalline structure of PLA inhibits the DOX entrapment in the inner cores. The averaged diameter of DOX-loaded P(IPAM–DMAM)/PLA micelles was 135 nm in a typical range of dispersed polymeric micelles (Fig. 2(b)). This result was probably due to that successful structural stabilization of thermoresponsive micelles was achieved by introduction of hydrophilic comonomer, DMAM into PIPAM main chains. For passive targeting using particles, their nano-ordered sizes (5–200 nm) are a very important factor for long circulation in the blood stream, avoiding from RES uptake [4], and allowing for selective tumor targeting due to the EPR effect of solid tumors. The prepared P(IPAM–DMAM)/PLA micelles have appropriate particle sizes with highly dispersed, non-aggregating properties, indicating their utility as targeted carrier systems.

The LCST of the DOX-loaded micelles were investigated by a turbidity method. In our previous works, it was clearly demonstrated that the hydrophilic or hydrophobic contribution to the LCST of PIPAM was particularly high when such groups were located at termini of the PIPAM chains [19,20]. The obtained hydroxyl-terminated PIPAM (PIPAM–OH) exhibited higher LCST of 34.5 °C in water than IPAM homopolymers prepared by conventional radical polymerization (32 °C). This

Table 1
Characterization of PIPAM-*b*-PBMA and the DOX-loaded micelles

Mw (PIPAM–OH)[a]	Mn (PBMA–COOH)[b]	LCST (°C)[c]	DOX content (wt%)
6100	8900	32.5	9.6

[a] Mw of PIPAM was determined by GPC in DMF with 10 mM LiCl.
[b] Mn of PBMA was estimated by end-group assay.
[c] Determined by transmittance changes in water.

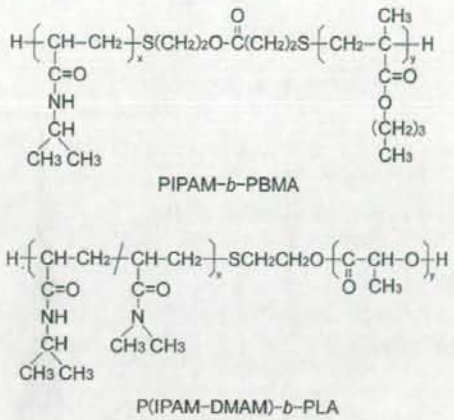

Fig. 1. Chemical structures of block copolymers.

result was considered that large hydrophilic contribution was enhanced by introduction of the terminal hydroxyl group in PIPAM due to stronger hydrogen bonding with water. However, the micelles comprising PIPAM-*b*-PBMA block copolymers showed the same LCST of unmodified IPAM homopolymers, irrespective of hydrophobic PBMA co-introduction. We have previously reported that thermoresponsive polymeric micelles comprising AB block copolymers of the PIPAM segment and a hydrophobic segment showed an LCST of 32.5 °C, identical to that of the IPAM homopolymer due to a clearly phase-separated micelle structure between the hydrophilic outer shells and the hydrophobic inner cores [19,21]. Furthermore, we have successfully adjusted the LCST of polymeric micelles comprising P(IPAM–DMAM)-*b*-PLA block copolymers to a temperature (39.5 °C) which is slightly higher than the body temperature by introduction of DMAM into the PIPAM main chain. This P(IPAM–DMAM)/PLA micelle system can be useful for multi-targeting methodology in conjunction with the localized hyperthermia at 42 °C, tumors are attacked by both selective cytotoxic activity of drugs (control of timing and duration) and selective hyperthermia [22].

3.3. Intracellular drug distribution

Subcellular distributions of DOX as free drug or loaded in the polymeric micelles inside of the cultured MCF-7 cells were observed by fluorescence microscopy detecting DOX fluorescence (red color). The nuclei of MCF-7 cells were selectively visualized (blue color) by Hoechst 33258 stain (Fig. 3(a and g)). Un-incorporated free DOX was almost exclusively found in nuclei (Fig. 3(b–f)) for incubation periods of 1 h to 24 h. The accumulation of free DOX progressed at a very high rate and saturated at 3 h incubation. For longer incubation periods, nuclei red color did not change. This behavior was identical to results reported in other papers [23]. Then, it was shown that subcellular distribution of DOX was not affected by temperature change from 37 °C (Fig. 4(a)) to 29 °C (Fig. 4(b)). On the other hand, DOX-loaded in the PIPAM/PBMA micelle system (LCST: 32.5 °C) was allowed to be clearly detected at 3 h and later. The intensity of the DOX color kept increasing by 24 h at a slower rate than free DOX (Fig. 3(h–l)). For the micelles, DOX images were shown to be uniformly distributed in whole inside of cells at 37 °C (above the micelle LCST) after thoroughly rinsing the cells to remove the micelles adhered to the cell surfaces below the LCST (25 °C). These results suggested that drug

Table 2
Characterization of P(IPAM–DMAM)-*b*-PLA and the DOX-loaded micelles

P(IPAM–DMAM)-*b*-PLA (P(IPAM–DMAM)–OH)[a]		Composition (molar ratio)[b]			LCST (°C)[c]	DOX content (wt%)
Mw[a]	PDI[a]	IPAM	DMAM	LA		
19600 (14800)	1.42 (1.26)	47	21	33	39.5	4.4

[a] Determined by GPC in DMF with 10 mM LiCl.
[b] Estimated by ^{1}H NMR spectrum.
[c] Determined by transmittance changes in PBS.

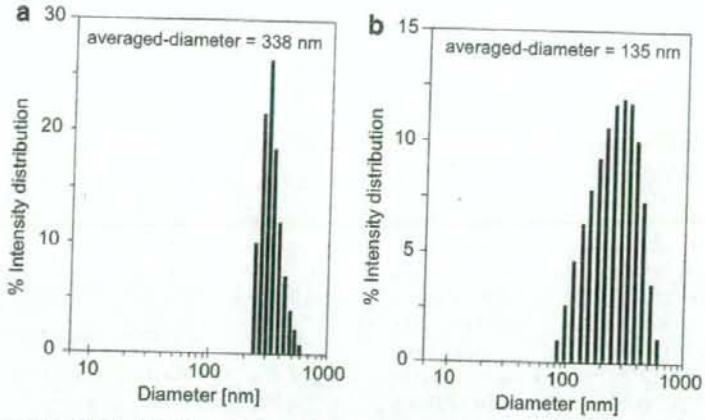

Fig. 2. Diameter distributions of (a) the DOX-loaded PIPAM/PBMA micelles and (b) the DOX-loaded P(IPAM–DMAM)/PLA micelles.

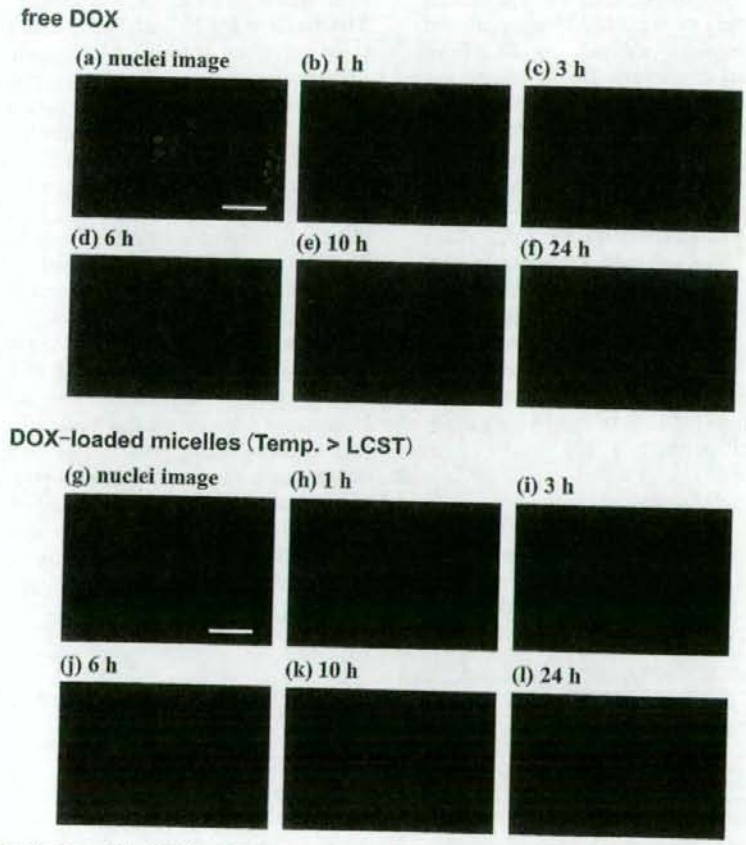

Fig. 3. Intracellular localization of free DOX and DOX-loaded in the PIPAM/PBMA micelles in MCF-7 cells. (a) nuclei stained with Hoechst 33258. Incubation for (b) 1 h, (c) 3 h, (d) 6 h, (e) 10 h and (f) 24 h with 30 μg/ml free DOX at 37 °C., (g) nuclei stained with Hoechst 33258. Incubation for (h) 1 h, (i) 3 h, (j) 6 h, (k) 10 h and (l) 24 h with 30 μg/ml DOX-loaded in the PIPAM/PBMA micelles at 37 °C. Bar represents 50 μm.

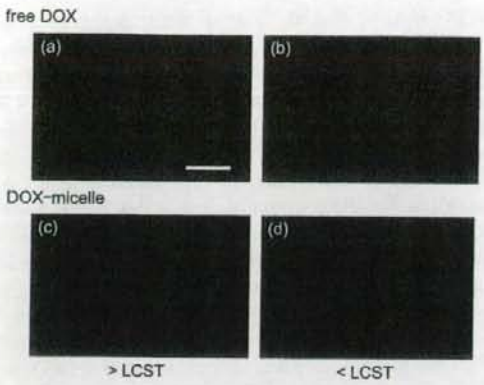

Fig. 4. Temperature effects on intracellular localization of DOX in MCF-7 cells.: Incubation for 6 h with 30 μg/ml free DOX at (a) 37 °C and (b) 29 °C. Incubation for 24 h with 30 μg/ml DOX loaded in the PIPAM/ PBMA micelles at (c) 37 °C and (d) 29 °C. Bar represents 50 μm.

delivery mechanism into the cells was different between free DOX and the DOX-loaded in the polymeric micelles. It is considered that DOX entered the cells in a micelle form, since its uniform distribution was totally different from free DOX distribution shown above. We have previously investigated temperature-modulated cellular uptake of fluorescein-labeled thermoresponsive micelles (averaged diameter: 30 nm) using cultured bovine endothelium cells by confocal laser scanning microscopy and flow cytometry [24]. Only above the micelle LCST, the micelles were significantly observed inside of the cells and localized around the nuclei. Furthermore, we have successfully achieved ON–OFF controlled intracellular uptake of the micelles via heating-cooling cycles across the micelle LCST. The drugs located at the nuclei using the micelles were probably due to accumulation of the released DOX from the micelles. In our previous report, the PIPAM/PBMA micelles exhibited approximately 90% DOX released against total loading content in PBS after 24 h above the LCST [15]. Of interest, as compared with images obtained above the LCST of the micelle (37 °C), the amount of DOX delivered to the cells drastically decreased below the LCST (29 °C) (Fig. 4(c and d)). This significant temperature effect indicated that hydrophilic PIPAM outer shells below its LCST lowered interactions with cell surfaces due to their highly hydrated shells. Upon the temperature raise above the micelle LCST, the outer shells switches their properties from hydrophilic to hydrophobic, and then the hydrophobic interactions between the micelles and the cell were consider to increase. Consequently, adhesion of the polymeric micelles was promoted, followed by significant enhancement of cellular uptake. Above the LCST, PIPAM-brush interfaces actively interact with biocomponents such as cells and proteins, whereas the surfaces changed into hydrated state with inhibiting these interactions below the LCST. Indeed, we have already demonstrated the PIPAM-grafted interfaces with a hydrophilic/hydrophobic switchable character for various applications including novel aqueous chromatography systems to separate bioactive compounds [25,26] and thermally regulated cell adhesion and detachment controlled solely by temperature changes [27,28].

We further investigated intracellular drug delivery *via* the thermoresponsive polymeric micelles using doxorubicin-resistant MCF-7 cell line (MCF-7/DOX). Free DOX was demonstrated much lower intracellular distribution in the resistant cells than its parent sensitive MCF-7 (Fig. 4(a) and Fig. 5(a)). This decrease is considered to result from efflux pump activity of the resistant cells. Interestingly, for the PIPAM/PBMA polymeric micelles above the micelle LCST, strong DOX fluorescence was observed in the DOX-resistant cells, irrespective of drug efflux activity. The extent of DOX intensity decreased only slightly compared with the DOX-

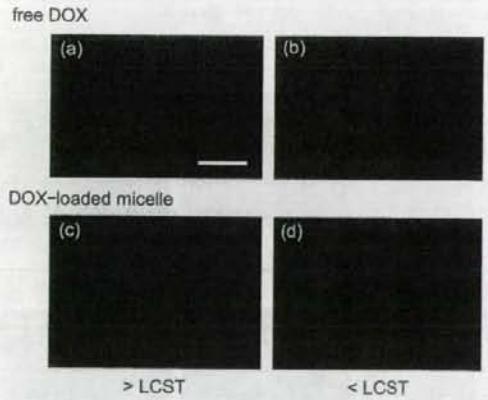

Fig. 5. Differences in intracellular localization between free DOX and DOX-loaded in the polymeric micelles in MCF-7 DOX resistant cells. Incubation for 6 h with 30 μg/ml free DOX at (a) 37 °C and (b) 29 °C. Incubation for 24 h with 30 μg/ml DOX-loaded in the PIPAM/PBMA micelles at (c) 37 °C and (d) 29 °C. Bar represents 50 μm.

sensitive cells (Fig. 4(c) and Fig. 5(c)). At the temperature below the LCST, the fluorescence intensity of DOX using the polymeric micelles was very small in this MCF-7/DOX. These results indicated that accumulation of free DOX was greatly inhibited in the resistant cell due to its resistant mechanism, and that a very large amount of drugs were delivered into the DOX-resistant cells utilizing thermal triggered micelle system. Consequently, we might accomplish to deliver anti-cancer drugs into MCF-7/DOX cells efficiently to overcome multi-drug resistant activity, and a novel strategy of cancer chemotherapy can be developed using the thermoresponsive micelle drug carrier system.

Biodegradable characters of the core-forming segments are preferable since the polymers obtained after the degradation (their molecular weights are below the critical value of ca. 40,000) can be rapidly excreted from the body through the renal excretion [29]. In addition, the thermoresponsive polymeric micelles with controlled higher LCST than human body temperature can be utilized for tumor hyperthermic treatment. Hyperthermia is known that exposure of high temperatures (around 42 °C) damages and kills cancer cells without biological damage to normal cells [22]. Therefore, we designed and prepared the P(IPAM–DMAM)/PLA micelles which possess both biodegradable properties of PLA inner cores and the controlled LCST value of 39.5 °C for the combination with the localized hyperthermic therapy. Intracellular distribution of free DOX at 37 °C and 42.5 °C was found to be effective the same as those in the experiment mentioned above (Fig. 3(b–f)). Free DOX was selectivity found in cell nuclei, and its red color was saturated at 6 h because no change was seen at 10 h and 24 h (data not shown). No temperature effect was observed between 37 °C and 42.5 °C. For the DOX-loaded in the P(IPAM–DMAM)/PLA micelles, the DOX accumulation in MCF-7 is much slower than free drug, it increased by 24 h incubation in a time-dependent manner (Fig. 6). In addition, the significant temperature effect of DOX accumulation across its LCST was clearly demonstrated using the thermoresponsive micelles. After 24 h incubation, a much larger amount of DOX in the cell above the LCST was detected than that below the LCST (Fig. 6(f and h)). In the P(IPAM–DMAM)/PLA micelle system, we also successfully controlled the critical temperature of intracellular drug delivery higher body temperature by LCST regulation of shell-forming polymer chains *via* hydrophilic DMAM introduction. Therefore, efficient tumor treatments can be obtained using thermoresponsive micelle drug carrier system in conjunction with local heating; tumor tissues are attacked by both selective cytotoxic activity of drugs and selective hyperthermia (42 °C). These phenomena of drug distribution using the thermoresponsive micelles were scarcely affected on differences in chemical components of block copolymers between two types of the micelles.

In order to confirm intracellular localization of free DOX and DOX loaded in the micelles, we

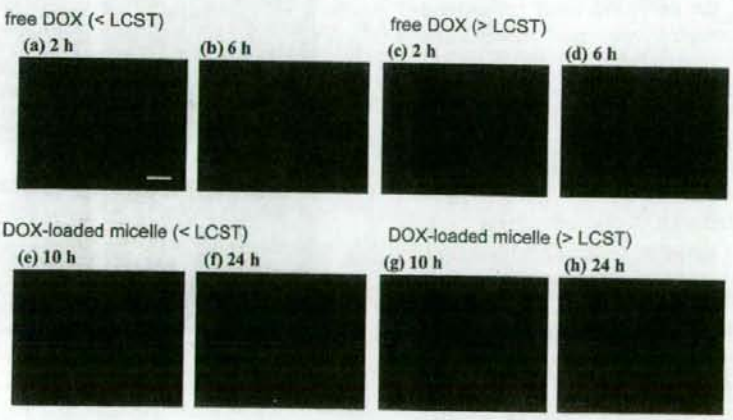

Fig. 6. Intracellular localization of free DOX and DOX-loaded in the P(IPAM–DMAM)/PLA micelles in MCF-7 cells. Incubation with 30 μg/ml free DOX for 6 h at (a) 37 °C and (b) 42.5 °C. Incubation with 30 μg/ml DOX-loaded in the P(IPAM–DMAM)/PLA micelles for 10 h at (c) 37 °C and (d) 42.5 °C, for 24 h at (e) 37 °C and (f) 42.5 °C. Bar represents 50 μm.

observed confocal images of MCF-7 cells exposed to each DOX. Free DOX was found to accumulate in only the cell nuclei (Fig. 7(a)). Kiyokami et al. previously reported the mechanism of selective DOX accumulation in the cell nuclei [30]; cytoplasmic DOX-binding proteasomes selectively transport DOX from the cytoplasm to the nucleus. By contrast, subcellular distribution of DOX using the micelles was observed in whole cells above its LCST as shown in Fig. 7(b). DOX accumulated in the cell nuclei using the thermoresponsive micelles probably due to accumulation of released DOX from the micelles. The P(IPAM–DMAM)/PLA micelles previously demonstrated 10% released against total loading DOX after 2 days in PBS above the LCST [17]. These suggested that DOX was mainly delivered into the cells in micelle form, and was enhanced intracellular release trough triggered phase transition of the micelle outer shells. Fig. 8 illustrates active drug targeting using the thermoresponsive polymeric micelles. We have previously demonstrated a thermal cytotoxic regulation using the DOX-loaded thermoresponsive micelles against cultured cell lines [15,17]. Expression of drug activity is initiated by external supply of heat. A delivery way of drug mediated by the temperature changes is considered the following two modes; (a) Drugs are extracellularly released from the polymeric micelles and diffuse into the cells, and (b) the polymeric micelles are taken up by the cells, and drugs are intracellularly released. It can be determined by a balance between the drug release rate and the frequency of cellular uptake which way plays a major role.

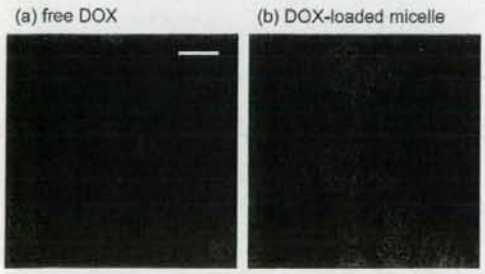

Fig. 7. Confocal images of free DOX and DOX-loaded in the P(IPAM–DMAM)/PLA micelles in MCF-7 cells. (a) Incubation with 30 μg/ml free DOX for 6 h at 42.5 °C, and (b) incubation with 30 μg/ml DOX-loaded in the P(IPAM–DMAM)/PLA micelles for 24 h at 42.5 °C. Bar represents 20 μm.

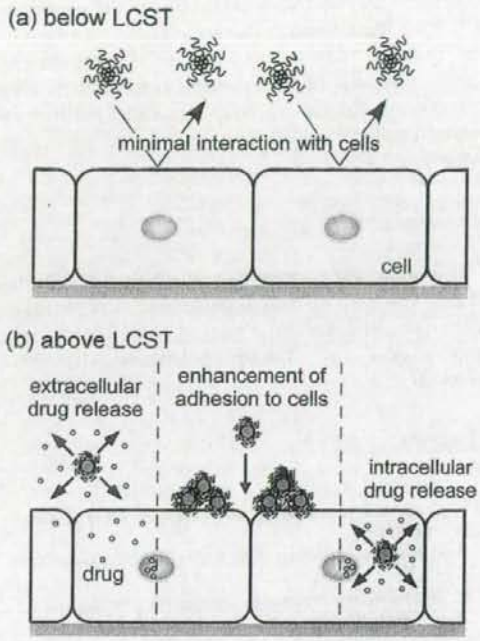

Fig. 8. Schematic mechanism of drug delivery to the target cells using the thermoresponsive polymeric micelles.

4. Conclusion

In this paper, we demonstrated the thermal modulation of intracellular drug distributions using the polymeric micelles with thermoresponsive outer shells comprising PIPAM or its copolymers. Unincorporated free DOX accumulated rapidly and selectively in cell nuclei without any temperature effects. By contrast, the distributions of DOX-loaded in the thermoresponsive micelles inside of the MCF-7 cells showed a significant temperature effect. DOX delivered by the micelles distributed uniformly in whole cells above the micelle LCST, while slight DOX accumulation was showed in the cell below the LCST. Interestingly, the DOX-loaded polymeric micelles exhibited a completely different behavior from free DOX in DOX-resistant MCF-7 cells. Although free DOX was detected slightly in the DOX resistant cells, the DOX-loaded in the micelles accumulated considerably above the LCST, irrespective of drug resistant activity. The thermal modulations of intracellular drug delivery using the thermoresponsive micelles also successfully achieved around human body temperature *via*

controlled micelle LCST (39.5 °C) for the combination with hyperthermic therapy. These results suggest that our thermoresponsive micelle system has a great potential in regulation of intracellular drug delivery against cancer cells including multi-drug resistant cells as well as for a multi-targeting cancer therapy.

Acknowledgement

This work was supported by the Ministry of Education, Culture, Sports, Science and Technology, Japan (a Millennium Project No. 12415 and Grant-in-Aid for Young Scientists (B) No. 19700407).

References

[1] D. Putnum, J. Kopecek, Adv. Polym. Sci. 122 (1995) 55.
[2] R. Duncan, S. Dimitrijevic, E.G. Evagoroa, S.T.P. Pharma. Sci. 6 (1996) 237.
[3] P.G. Tardi, N.L. Boman, P.R. Cullis, J. Drug Targeting 4 (1996) 129.
[4] O. Ishida, K. Maruyama, K. Sasaki, M. Iwatsuru, Int. J. Pharm. 190 (1999) 49.
[5] G.S. Kwon, K. Kataoka, Adv. Drug Deliv. Rev. 16 (1995) 295.
[6] Z. Tuzar, P. Kratochvil, Adv. Colloid Interf. Sci. 6 (1976) 201.
[7] M. Wilhelm, C. Zhao, Y. Wang, R. Xu, M.A. Winnik, J. Mura, G. Riess, M.D. Croucher, Macromolecules 24 (1991) 1033.
[8] Y. Matsumura, H. Maeda, Cancer Res. 46 (1986) 6387.
[9] H. Maeda, L.W. Seymour, Y. Miyamoto, Bioconjugate Chem. 3 (1992) 351.
[10] G.S. Kwon, S. Suwa, M. Yokoyama, T. Okano, Y. Sakurai, K. Kataoka, J. Control. Release 29 (1994) 17.
[11] M. Yokoyama, T. Okano, Y. Sakurai, S. Fukushima, K. Okamoto, K. Kataoka, J. Drug Targeting 7 (1999) 171.
[12] M. Nakayama, T. Okano, J. Drug Deliv. Sci. Tech. 16 (2006) 35.
[13] Z.-G. Gao, H.D. Fain, N. Rapoport, J. Control. Release 102 (2005) 203.
[14] K. Na, E.S. Lee, Y.H. Bae, J. Control. Release 87 (2003) 3.
[15] J.E. Chung, M. Yokoyama, M. Yamato, T. Aoyagi, Y. Sakurai, T. Okano, J. Control. Release 62 (1999) 115.
[16] F. Kóhori, K. Sakai, T. Aoyagi, M. Yokoyama, Y. Sakurai, T. Okano, J. Control. Release 55 (1998) 87.
[17] F. Kohori, K. Sakai, T. Aoyagi, M. Yokoyama, M. Yamato, Y. Sakurai, T. Okano, Colloids Surf. B: Biointerf. 16 (1999) 195.
[18] M. Heskins, J.E. Guillet, J. Macromol. Sci. Chem. A2 (1968) 1441.
[19] J.E. Chung, M. Yokoyama, T. Aoyagi, Y. Sakurai, T. Okano, J. Control. Release 53 (1997) 119.
[20] J.E. Chung, M. Yokoyama, K. Suzuki, T. Aoyagi, Y. Sakurai, T. Okano, Colloids Surf. B: Biointerf. 9 (1997) 37.
[21] S. Cammas, K. Suzuki, Y. Sone, Y. Sakurai, K. Kataoka, T. Okano, J. Control. Release 48 (1997) 157.
[22] A.M. Ponce, Z. Vuujaskovic, F. Yuan, D. Needham, M.W. Dewhirst, Int. J. Hyperthermia 22 (2006) 205.
[23] O. Hovorka, M. St'astny, T. Etych, V. Subr, J. Strohalm, K. Ulbrich, B. Rihova, J. Control. Release 80 (2002) 101.
[24] J. Akimoto, M. Nakayama, K. Sakai, T. Okano, Submitted for publication.
[25] H. Kanazawa, T. Sunamoto, Y. Matsushima, A. Kikuchi, T. Okano, Anal. Chem. 72 (2000) 5961.
[26] J. Kobayashi, A. Kikuchi, K. Sakai, T. Okano, Anal. Chem. 73 (2001) 2027.
[27] T. Okano, N. Yamada, H. Sakai, Y. Sakurai, J. Biomed. Mater. Res. 27 (1993) 1243.
[28] T. Okano, N. Yamada, M. Okuhara, H. Sakai, Y. Sakurai, Biomaterials 16 (1995) 297.
[29] L.W. Seymour, R. Duncan, J. Strohalm, J. Kopecek, J. Biomed. Mater. Res. 21 (1987) 1341.
[30] K. Kiyokami, S. Matsuo, M. Kurebe, Cancer Res. 61 (2001) 2467.

A novel synthetic tissue-adhesive hydrogel using a crosslinkable polymeric micelle

Yoshihiko Murakami,[1] Masayuki Yokoyama,[1] Teruo Okano,[2] Hiroshi Nishida,[3] Yasuko Tomizawa,[3] Masahiro Endo,[3] Hiromi Kurosawa[3]

[1]*Yokoyama Nano-Medical Polymer Project, Kanagawa Academy of Science and Technology (KAST), KSP East 404, Sakado 3-2-1, Takatsu, Kawasaki, Kanagawa 213-0012, Japan*

[2]*Institute of Advanced Biomedical Engineering and Science, Tokyo Women's Medical University, 8-1 Kawada-cho, Shinjuku-ku, Tokyo 162-8666, Japan*

[3]*Department of Cardiovascular Surgery, The Heart Institute of Japan, Tokyo Women's Medical University, 8-1 Kawada-cho, Shinjuku, Tokyo 162-8666, Japan*

Received 20 February 2006; revised 17 March 2006; accepted 3 May 2006
Published online 29 September 2006 in Wiley InterScience (www.interscience.wiley.com). DOI: 10.1002/jbm.a.30911

Abstract: We prepared a novel tissue-adhesive hydrogel by using a polymeric micelle consisting of an aldehyde-terminated poly(ethylene glycol)–poly(D,L-lactide) (PEG–PLA) block polymer. A Schiff base is chemically formed between the amino groups in a polyallylamine and the aldehyde groups on the surface of polymeric micelles. The hydrogel was formed in ~2 s when the polymeric micelle solution and polyallylamine solution are mixed *in vitro*. The hydrogel was rapidly formed *in vivo*, and it adhered to a tissue surface. Our novel tissue-adhesive hydrogel creates no risk of infectious contaminations, because it consists of only synthetic materials. Further, PEG and PLA are known to be biocompatible and noncytotoxic. The results obtained in the present study show that a hydrogel prepared by the formation of a Schiff base between aldehyde and amine groups will potentially address the need for novel tissue-adhesive materials. © 2006 Wiley Periodicals, Inc. J Biomed Mater Res 80A: 421–427, 2007

Key words: tissue-adhesive hydrogel; polymeric micelle; block polymer; polyethylene glycol; polylactide

INTRODUCTION

Tissue-adhesive materials are clinically used for local hemostasis in surgery and for stopping body fluid and air leaks that may be resistant to conventional suture or stapling techniques. In the past few decades, several tissue-adhesive formulations have been developed. These include fibrin glues,[1,2] collagen sheets with fibrin glues,[3] fibrillar collagen,[4] collagen with citric acid derivative,[5] gelatin with resorcin and formalin (GRF glue™),[6] albumin with glutaraldehyde,[7] cyanoacrylate,[8] and synthetic polymers.[9–12] However, these materials have a number of disadvantages and need to be improved for clinical use.

Fibrin-based glues have been widely used in a variety of surgical procedures and are designed to mimic the physiology of the final steps of the blood coagulation cascade. However, there is a risk of infectious contaminations when these glues are used. Collagen and gelatin are not suitable as tissue-contacting materials owing to the same risk factor, although they are known to possess beneficial characteristics—high tensile strength, absorbability in the body, and good cell compatibility. A systemic allergic reaction was reported when collagen-based hemostat was used in a laparoscopic cholecystectomy.[13] Furthermore, the glues that contain these aldehydes as crosslinkers are highly cytotoxic, because aldehydes with low molecular weights (such as formaldehyde and glutaraldehyde) deeply penetrate tissues owing to their high diffusive characteristics.

Synthetic glues have been actively developed because they do not possess the risk of infectious contaminations. Cyanoacrylate is comparable to fibrin glues, but it offers additional benefits such as a relatively high bonding strength and no risk of infectious contaminations. However, its cytotoxicity and lack of biodegradability restrict its use. On the other hand, synthetic polymer-based glues have beeneasily syn-

Correspondence to: M. Yokoyama; e-mail: masajun@ksp.or.jp
Contract grant sponsor: Ministry of Education, Culture, Sports, Science and Technology of Japan

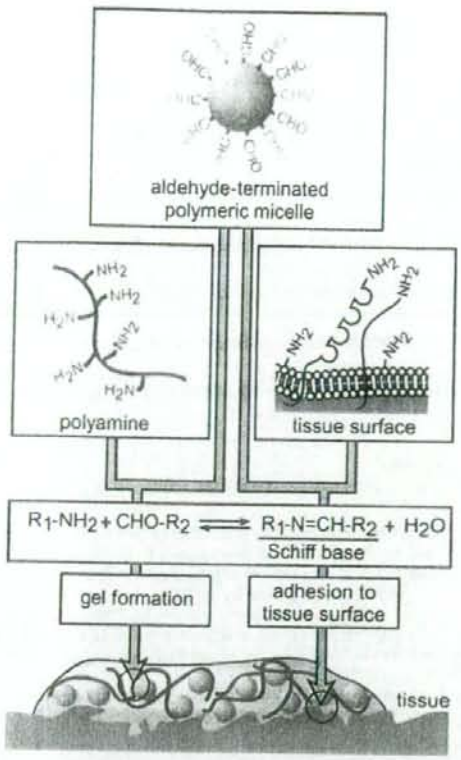

Figure 1. Novel synthetic tissue-adhesive hydrogel that uses a crosslinkable polymeric micelle.

thesized with a molecular design that controls their absorbability, biodegradability, and reactivity, thus making them promising biomaterials. They are polymerized by using photoreactive[9,10] or reactive[11,12] monomers. However, photoactivation makes application of the glue quite difficult and nearly impossible in case of a hemorrhage.

We propose a novel synthetic tissue-adhesive hydrogel that uses a crosslinkable polymeric micelle (Fig. 1). A Schiff base is chemically formed between the amino groups in a polyamine (e.g. polyallylamine) and the aldehyde groups on the surface of a polymeric micelle. A polymeric micelle is a macromolecular spherical particle (molecular weight: ca. 3000–4000 kDa) that is formed from block or grafted polymers in which the hydrophilic and hydrophobic blocks are combined. PEG is known to be biocompatible, because the interaction between PEG and cells is quite low. Actually, the poly(ethylene glycol) (PEG)-based hydrophilic blocks form the shell that helps the micelle to stay unrecognized during blood circulation in drug delivery systems.[14] We can easily transform the micelle into a highly reactive crosslinker by using aldehyde-terminated block polymers. This highly reactive crosslinker may give a fast gelation property to the polymeric micelle-based glue, which is an important property for hemostasis. Owing to these properties, a polymeric micelle can be used as a macromolecular and biocompatible crosslinker in our novel hydrogel. The resulting hydrogel can be expected to adhere to a tissue because of the Schiff base formation between the aldehyde groups on the surface of a polymeric micelle and the amino groups that are present on the tissue surface (e.g. primary amino groups of cell adhesion molecules and lipids).

In the present article, we describe the preparation of a novel hydrogel, the effect that the properties of polymer solutions have on both the hydrogel strength and the gelation time, and the tissue-adhesive properties of the hydrogel to the peritoneum of mice.

MATERIALS AND METHODS

Materials

An acetal-terminated PEG–poly(D,L-lactide) (PEG–PLA) block polymer (1, Fig. 2) was synthesized according to a reference.[15] We obtained acetal-terminated PEG–PLA by employing anionic ring-opening polymerization from ethylene oxide and D,L-lactide in tetrahydrofuran. After the reaction, the block polymer was precipitated into cold 2-propanol and lyophilized in benzene. The number-average molecular weights of the acetal-terminated block polymer was 9470 (PEG and PLA units were 5310 and 4010, which were

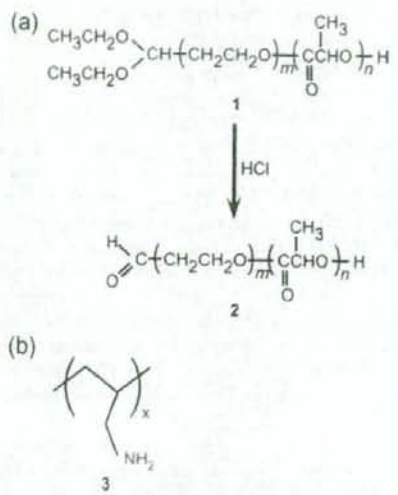

Figure 2. Molecular structure of the polymers, (a) acetal-terminated poly(ethylene glycol-*block*-D,L-lactide) and (b) polyallylamine, used in this study.

determined on the basis of a gel permeation chromatography and ^{1}H NMR, respectively). ^{1}H NMR also showed that the acetal group was introduced to 92.6% of the terminus of the polymer. Polyallylamine (3) hydrochloride with average molecular weights of 5000, 15,000, 60,000, and 150,000 were generously provided by Nitto Boseki (Japan) and were used as a polyamine component. All the other reagents were of analytical grade and were used without further purification.

Preparation of an aldehyde-terminated polymeric micelle

Two-types of polymeric micelles were prepared. One consisted of aldehyde (100 w/w%)-terminated PEG–PLA (2) and the other consisted of aldehyde (10 w/w%)/acetal (90 w/w%)-terminated PEG–PLA. We dissolved the acetal-terminated PEG–PLA in *N,N*-dimethylacetamide, and then performed dialysis against water by using a Spectra/Por7 dialysis membrane (molecular weight cut-off: 1 kDa; Spectrum, Houston, TX) for 24 h. We stirred the polymeric micelle solution at pH 2 for 2 h after adding HCl to convert the acetal group into the aldehyde group on the surface of the micelle. To stop the reaction, we adjusted the solution to pH 5 by adding NaOH. The polymeric micelle that consisted of only aldehyde-terminated PEG–PLA was finally obtained through dialysis against water for 24 h, which made possible the removal of the salt. We also prepared the polymeric micelle that consisted of aldehyde (10 w/w%)/acetal (90 w/w%)-terminated PEG–PLA by mixing both the lyophilized polymeric micelle containing only aldehyde-terminated PEG-PLA (obtained earlier) and acetal-terminated PEG–PLA (10/90, w/w) in *N,N*-dimethylacetamide. Following this step, we performed dialysis against water for 24 h. We adjusted the solution to pH 5 by adding NaOH and dialyzed against water for 24 h for the removal of the salt. We concentrated the solution by evaporating at 50–60°C.

In vitro hydrogel formation

The solutions containing either a polymeric micelle (10 or 17 w/w%, pH 5, 0.25 mL) or polyallylamine (0.5–2.0 w/w%, pH 6–9 which was adjusted by HCl/NaOH, 0.25 mL) were mixed in a glass vial (length: 2 cm and inner diameter 1.6 mm) at 37°C. The hydrogel strength and the gelation time were then evaluated. The time period required for the magnetic stirring bar to stop stirring was defined as the gelation time of the mixed solution.[16] We observed the fluidity of the hydrogel from the top of the vial to the bottom by setting the vial in an inverted position after hydrogel formation. Using a coagulometer (Biomatic B10 model; Sarstedt, UK), we determined the gelation properties of the hydrogel by mixing the solutions containing either a polymeric micelle (10 or 17 w/w%, pH 5, 0.25 mL) or polyallylamine (0.5–2.0 w/w%, pH 6–9, 0.25 mL). We obtained the calibration curve by using a glycerine solution (60–90 w/w%) whose viscosity was determined via a viscosity meter VM-1G (Nikkato, Osaka, Japan).

In vivo hydrogel formation

Pentobarbital sodium (Nembutal™, Dainippon Pharmaceutical, Japan) was injected intraperitoneally into ddY mice. We performed celiotomy by creating an abdominal incision. By using tweezers to move the hydrogel, we evaluated the ability of the hydrogel to adhere to the peritoneum of mice. We used the following two methods to form the hydrogel—Method A: The solutions containing either a polymeric micelle (18 w/w%, pH 5) or polyallylamine (2.0 w/w%, at pH 9) were simultaneously applied to the peritoneum of mice. For this method, we used a two-pronged needle that consisted of two syringes and that is commonly used for the application of commercially available tissue-adhesive, namely, BOLHEAL™ (Kaketsuken, Japan) in order to mix two solutions. Method B: The solutions containing either a polymeric micelle (18 w/w%, pH 5) or polyallylamine (2.0 w/w%, pH 6) were mixed *in vitro* and were applied to the peritoneum of mice. Then an addition of sodium carbonate, wherein hematoxylin was solubilized (7.0 w/w%, pH 11.5), increased the pH. It is difficult to measure the final pH in Method B *in vivo*, since it was observed that the whole applied volume of a sodium carbonate solution (pH 11.5) was not used due to a low viscosity of this solution (most volume of the solution dispersed on the tissue without being used for an increase in pH of the more viscous solution of the polymeric micelle and the polyallylamine). We performed a control experiment by using commercially available fibrin glue, namely, Beriplast™ (Aventice Behring, Germany).

RESULTS AND DISCUSSION

In vitro hydrogel formation by a magnetic stirring

There still remains a clinical need for effective tissue-adhesive glues, even though numerous tissue-adhesive materials have been proposed and tested preclinically and clinically. One of the desired features of tissue-adhesive glues is reduced gelation time, that is, gelation within a few seconds. The gelation time and the hydrogel strength of our novel hydrogel are shown in Table I. The hydrogel was rapidly formed when the polymeric micelle solution and the polyallylamine solution were mixed under the experimental conditions with a few exceptions. The time required for hydrogel formation (2 s) was comparable to or shorter than that previously reported for other tissue-adhesive hydrogels. This property of the hydrogel is important from the viewpoint of its clinical applications. It is difficult to form a hydrogel on a tissue surface when the time required for *in vivo* hydrogel formation is long because the polymeric micelle solution and the polyallylamine solution gradually disperse before the hydrogel is completely formed.

We obtained the hydrogel by forming—in a pH-dependent manner—the Schiff base. No hydrogel formation was observed when the polyallylamine solution at pH 6 was used (entry 1), whereas hydrogel was formed when the pH of the polyallylamine solution was higher than 7 (entries 2–6) (entry codes are shown in the tables). The hydrogel was formed in ~2 s in the latter cases. However, there is a subtle difference in

TABLE I
Properties of the Tissue-Adhesive Hydrogel Formed *In Vitro*

Entry	Concentration of Polymeric Micelle (w/w%)	Polyallylamine		pH (–)	Hydrogel Strength[a]	Gelation Time (s)[b]
		Molecular Weight (g/mol)	Concentration (w/w%)			
1	10	150,000	1.0	6.0	–	–
2	10	150,000	1.0	7.0	+++	<2
3	10	150,000	1.0	7.5	+++	<2
4	10	150,000	1.0	8.0	+++	<2
5	10	150,000	1.0	8.5	+++	<2
6	10	150,000	1.0	9.0	+++	<2
7	10	150,000	2.0	8.0	+++	<2
8	10	150,000	0.5	8.0	+++	<2
9	10	60,000	1.0	8.0	++	<2
10	10	15,000	1.0	8.0	+	<2
11	10	5,000	1.0	8.0	–	–
12	17	150,000	1.0	8.0	+++	<2

[a]We observed the hydrogel's fluidity from the top to the bottom of the vial was observed by setting the vial in the inverted position after hydrogel formation (–, hydrogel was not formed; +, hydrogel rapidly moved to the bottom within 2 s; ++, hydrogel moved slowly; +++, hydrogel did not move).
[b]–, hydrogel was not formed.

each case: the hydrogel was gradually formed when the polyallylamine solution at pH 7 was used, whereas the gelation was slightly faster when the polyallylamine solutions at pH 8–9 were used. Schiff base formation ($R_1—NH_2 + CHO—R_2 \rightleftharpoons R_1—N=CH—R_2 + H_2O$) is faster at a slightly acidic pH: for instance, Schiff base formation between 5-formyluracil and 5-aminocytosine is faster at pH 5.8 than at pH 7.0.[17] However, because a primary amine obeys the equilibrium $R_1—NH_2 + H^+ \rightleftharpoons R_1—NH_3^+$, the concentration of reactive $R_1—NH_2$ thus increases as pH increases. Thus, there is an optimal pH for Schiff base formation. In our case, the hydrogel was rapidly formed when the polyallylamine solutions at pH 8 and 9 were used, whereas a white aggregate with a low gel strength was formed when the polyallylamine solution at a pH over 10 was used (data not shown). These findings indicate that the optimal pH for the formation of the Schiff base between polyallylamine and the aldehyde groups on the surface of a polymeric micelle is 8–9.

The hydrogel strength was greatly dependent on the molecular weight of polyallylamine. We evaluated hydrogel strength by observing the fluidity of the hydrogel from the top to the bottom of the vial by setting the vial in an inverted position. On the basis of the fluidity, the hydrogel strength was classified into four categories as follows: (+) hydrogel rapidly moved to the bottom within 2 s, (++) hydrogel moved slowly, (+++) hydrogel did not move, and (–) hydrogel was not formed. The hydrogel strength lowered as the molecular weight of the polyallylamine decreased (entries 4, 9–11). This outcome indicates that the main chain length of polyallylamine was an important factor in the regulation of a hydrogel strength. It become clear that when the molecular weight of polyallylamine was 150,000 and when the concentration of polyallylamine was 0.5–2.0 w/w%, the hydrogel strength was sufficiently high, thereby making the gel elastic (entries 2–8). The hydrogel did not move in the inverted vial when the concentration of the polymeric micelle was 17 w/w% (entry 12). We observed that, in this case, the gel strength was slightly higher than the gel strength that manifested itself when the concentration of the polymeric micelle was 10 w/w% (entry 4). Even in the former case, a gelation time was still short, and this finding indicates that the increase of the viscosity of a polymeric micelle solution did not influence the diffusion property of the polymeric micelle.

In vitro hydrogel formation by a coagulometer

We further evaluated the gelation properties by using a coagulometer that could detect the change in viscosity in a short time range (Table II), because the hydrogel formation that we induced by mixing the polymeric micelle solution and polyallylamine solution was rapid. A coagulometer can facilitate monitoring of the blood-clotting process by "tapping (not mixing)" a blood sample. Thus, for the application of the hydrogel *in vivo* in the next steps, a coagulometer-determined hydrogel gives rise to properties that are expected to be more useful than the properties that correspond to a hydrogel obtained via magnetic stirring (mentioned earlier). Figure 3 shows the typical time-course of the coagulometer-determined gelation (ca. 90 in the output value was the detection limit of the coagulometer). The solution showed the almost the same output value before the addition of a polymeric micelle solution (the solution was added at $t = 0$). However, once a polymeric micelle solution was added, the output value changed depending on the

TABLE II
Properties of the Tissue-Adhesive Hydrogel Formed *In Vitro* Determined by Coagulometer

Entry[a]	Concentration of Polymeric Micelle (w/w%)	Polyallylamine			Hydrogel Viscosity (mPa·s)	Time Required by the Hydrogel to Reach a Viscosity of 30 mPa·s
		Molecular Weight (g/mol)	Concentration (w/w%)	pH (–)		
2a	10	150,000	1.0	7.0	>40	3.0
3a	10	150,000	1.0	7.5	>40	2.0
4a	10	150,000	1.0	8.0	>40	2.0
5a	10	150,000	1.0	8.5	>40	2.0
6a	10	150,000	1.0	9.0	>40	1.7
7a	10	150,000	2.0	8.0	>40	1.5
8a	10	150,000	0.5	8.0	>40	3.3
9a	10	60,000	1.0	8.0	>40	1.4
10a	10	15,000	1.0	8.0	>40	1.6
11a	10	5,000	1.0	8.0	4	–[b]
12a	17	150,000	1.0	8.0	>40	1.3

[a]–, Entry numbers are consistent with those in Table I except an addition of "a". For example, entry 2a in Table II corresponds to entry 2 in Table I.
[b]–, hydrogel was not formed.

gelation property of the mixed solution obtained. Namely, the output value increased by a gelation (solid line in Fig. 3), whereas in the case when the hydrogel was not formed, the output value did not increase (dotted line in Fig. 3).

This coagulometer outputs the values in response to the resistance to the detection bar, which was induced by the change in the solution's viscosity. We thus determined the calibration curve by using a glycerine solution whose viscosity was already determined via a viscosity meter (Fig. 4). It is obvious that the upper detection limit of the coagulometer was 40 mPa·s in viscosity. Table II summarizes the gelation property of the mixed solution. The hydrogel showed almost the same viscosity in our experimental condition, except when the molecular weight of polyallylamine was low (entry 11a), indicating that the main chain should be sufficiently long to form a hydrogel. The gelation rate could be evaluated on the basis of the time required for the viscosity of the hydrogel to reach 30 mPa·s. The hydrogel formation was enhanced when either the pH of the polyallylamine solution was higher (a comparison of entries 3a–6a with entry 2a) or the concentration of the polyallylamine was higher (a comparison of entries 6a–7a with entry 8a). Although the gelation times, as evaluated according to the two methods, differed from each other owing to the difference in the gel-forming method (mixing or tapping), similar results were obtained (Tables I and II). The coagulometer-based evaluation clearly showed the gelation properties in a short time range that are important when the hydrogel is applied *in vivo*.

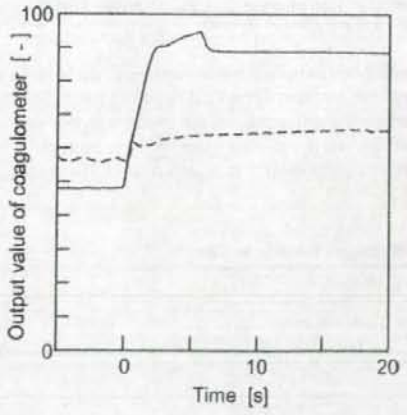

Figure 3. Typical time-course of the hydrogel determined by a coagulometer. The solid line shows the case when the hydrogel was formed (entry 4 in Table I), whereas the dotted line shows the case when the hydrogel was not formed (entry 11 in Table I).

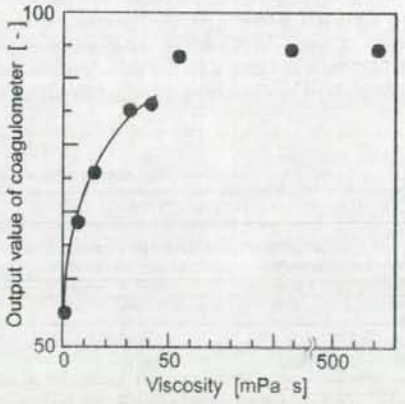

Figure 4. Calibration of coagulometer (output values of coagulometer were plotted against the viscosity of the solution).

Further optimization studies are currently being performed. As shown in Tables I and II, it is obvious that the formation of the Schiff base (depending on the pH) and the formation of the crosslinks (depending on the molecular weight and the concentration of the main chain-forming polymer and the concentration of the crosslinkable molecule) are important for the formation of the hydrogel proposed in this study.

In vivo hydrogel formation

We evaluated the hydrogel formation on the peritoneum of mice. The hydrogel was formed according to two methods. One method employed the simultaneous application of both the polymeric micelle and the polyallylamine solutions to the peritoneum of mice (Method A). The other method involved (1) the application of both the solution containing the polymeric micelle and polyallylamine to the peritoneum of mice and (2) the addition of sodium carbonate so that pH would increase (Method B). With Method A as well as Method B, the hydrogel was rapidly formed on the peritoneum of mice (Fig. 5, the hydrogel was slightly colored by hematoxylin for easy visualization in the latter case). The transparent and thin hydrogel adhered to a tissue surface.

We examined the effect that density of the aldehyde-terminated group had on the surface of the polymeric micelle. We used two types of polymeric micelles-one consisting of aldehyde (100 w/w%)-terminated PEG-PLA (entries 13 and 15) and the other consisting of aldehyde (10 w/w%)/acetal (90 w/w%)-terminated PEG-PLA (entries 14 and 16) (Table III). We performed a control experiment by using commercially available fibrin glue. We found that the hydrogel strength was sufficiently high, and that it therefore made the gel elastic. This was observed in all cases, independently of the density of the aldehyde-terminated group on the surface of the polymeric micelle. On the other hand, the adhesion strength of the hydrogel to the peritoneum of mice decreased as the density of the aldehyde-terminated group on the surface of the polymeric micelle decreased (entries 14 and 16). The currently

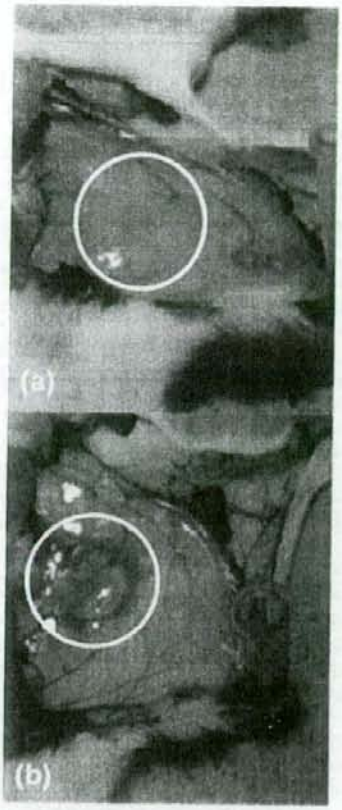

Figure 5. The hydrogel that adheres to the peritoneum of a mouse [(a) Method A and (b) Method B]. White circle shows the hydrogel formed.

available tissue-adhesive materials adhere to tissues because of the mechanical bonding provided by polymerized monomers, which penetrate the tissues in a soluble form during the polymerization ("anchor effect"). Although this is also true for the hydrogel pre-

TABLE III
Properties of the Tissue-Adhesive Hydrogel Formed *In Vivo*

	Polymeric Micelle		Polyallylamine					
Entry	Concentration (w/w%)	Aldehyde-Terminated Groups (w/w%)	Molecular Weight (g/mol)	Concentration (w/w%)	pH (–)	Method	Hydrogel Strength[a]	Adhesion Strength[b]
13	18	100	150,000	2.0	9.0	A	+++	+
14	18	10	150,000	2.0	9.0	A	+++	
15	18	100	150,000	2.0	6.0	B	+++	+
16	18	10	150,000	2.0	6.0	B	+++	–

[a]We observed the hydrogel's fluidity from the top to the bottom of the vial was observed by setting the vial in the inverted position after hydrogel formation (keys are the same as shown in Table I).
[b]+, Adhesion strength was comparable to that of the fibrin glue; –, adhesion strength was weaker than that of the fibrin glue.

pared in this study, the additional tissue-adhesive mechanism based on a chemical bonding has another advantage. As shown in Table III, the gel adhesion strength was affected by the density of the aldehyde-terminated group on the surface of the polymeric micelle, even though the hydrogel strength was independent of the density. This result suggests that the hydrogel adheres to tissues according to two mechanisms: (1) the Schiff base formation between the aldehyde groups in the polymeric micelles and the amino groups that are present on the tissue surface and (2) the conventional anchor effect-that is, mechanical bonding enables the gel to fit into the uneven surface of tissues.

CONCLUSIONS

We successfully prepared a novel tissue-adhesive hydrogel by using a crosslinkable polymeric micelle. The incorporation of the crosslinkable polymeric micelle into the hydrogel could make the micelle a novel biomaterial. Two solutions containing either a polymeric micelle or polyallylamine formed a hydrogel *in vivo* and *in vitro* immediately after these two solutions were mixed. The hydrogel adhered to the peritoneum of mice.

The novel hydrogel prepared in this study has some interesting features. It has been reported that aldehydes with low molecular weights as crosslinkers are cytotoxic because of their high permeability into tissue, thereby allowing them to penetrate tissues. For this study, we used a macromolecular crosslinker that was expected to have a low permeability into tissue. The components of polymeric micelles (PEG and PLA) are known to be noncytotoxic and biocompatible. Our novel adhesive does not carry the risk of transmission of infectious contaminations, because it consists of only synthetic materials. Although an aldehyde-terminated polymeric micelle has been one of the useful functional carriers in drug delivery systems,[18] it is necessary that future research test the biocompatibility of the hydrogel in detail. The evaluation of other polyamines (e.g. poly(amino acid) and chitosan) is now underway, because polyallylamine, which was used in this study, may not be the best choice as an amine component for medical use. Although quantitative investigations concerning hydorogel properties are necessary in the future, the preliminary results obtained in the present study show that a hydrogel prepared through a crosslinkable polymeric micelle has the potential to address the need for novel adhesives.

References

1. Morikawa T. Tissue sealing. Am J Surg 2001;182:29S–35S.
2. MacGillivray TE. Fibrin sealants and glues. J Card Surg 2003; 18:480–485.
3. Czerny M, Verrel F, Weber H, Muller N, Kircheis L, Lang W, Steckmeier B, Trubel W. Collagen patch coated with fibrin glue components. Treatment of suture hole bleedings in vascular reconstruction. J Cardiovasc Surg 2000;41:553–557.
4. Turner AS, Parker D, Egbert B, Maroney M, Armstrong R, Powers N. Evaluation of a novel hemostatic device in an ovine parenchymal organ bleeding model of normal and impaired hemostasis. J Biomed Mater Res (Appl Biomater) 2002; 63:37–47.
5. Taguchi T, Saito H, Uchida Y, Sakane M, Kobayashi H, Kataoka K, Tanaka J. Bonding of soft tissues using a novel tissue adhesive consisting of a citric acid derivative and collagen. Mater Sci Eng C 2004;24:775–780.
6. Fukunaga S, Karck M, Harringer W, Cremer J, Rhein C, Haverich A. The use of gelatin-resorcin–formalin glue in acute aortic dissection type A. Eur J Cardiothorac Surg 1999;15:564–570.
7. Kumar A, Maartens NF, Kaye AH. Evaluation of the use of BioGlue in neurosurgical procedures. J Clin Neurosci 2003;10: 661–664.
8. Singer AJ, Thode HC. A review of the literature on octylcyanoacrylate tissue adhesive. Am J Surg 2004;187:238–248.
9. Ramakumar S, Roberts WW, Fugita OE, Colegrove P, Nicol TM, Jarrett TW, Kavoussi LR, Slepian MJ. Local hemostasis during laparoscopic partial nephrectomy using biodegradable hydrogels: Initial porcine results. J Endourol 2002;16: 489–494.
10. Nakayama Y, Matsuda T. Photocurable surgical tissue adhesive glues composed of photoreactive gelatin and poly(ethylene glycol) diacrylate. J Biomed Mater Res (Appl Biomater) 1999;48: 511–521.
11. Ferland R, Mulani D, Campbell PK. Evaluation of sprayable polyethylene glycol adhesion barrier in a porcine efficacy model. Hum Reprod 2001;16:2718–2723.
12. Wallace DG, Cruise GM, Rhee WM, Schroeder JA, Prior JJ, Ju J, Maroney M, Duronio J, Ngo MH, Estridge T, Coker GC. A tissue sealant based on reactive multifunctional polyethylene glycol. J Biomed Mater Res (Appl Biomater) 2001;58:545–555.
13. Kitamura K, Yasuoka R, Ohara M, Shimotsuma M, Hagiwara A, Yamane T, Yamaguchi T, Takahashi T. How safe are the xenogeneic hemostats?—Report of a case of severe systemic allergic reaction. Surg Today 1995;25:433–435.
14. Yokoyama M. Drug targeting with nano-sized carrier systems. J Artif Organs 2005;8:77–84.
15. Scholz C, Iijima M, Nagasaki Y, Kataoka K. A novel reactive polymeric micelle with aldehyde groups on its surface. Macromolecules 1995;28:7295–7297.
16. Otani Y, Tabata Y, Ikada Y. A new biological glue from gelatin and poly(L-glutamic acid). J Biomed Mater Res 1996;31:157–166.
17. Dohno C, Okamoto A, Saito I. Stable, specific, and reversible base pairing via Schiff base. J Am Chem Soc 2005;127:16681–16684.
18. Nagasaki Y, Okada T, Scholz C, Iijima M, Kato M, Kataoka K. The reactive polymeric micelle based on an aldehyde-ended poly(ethylene glycol)/poly(lactide) block copolymer. Macromolecules 1998;31:1473–1479.

Journal of
Nanoscience and Nanotechnology
Vol. 8, 1–6, 2007

Polymeric Micelles Modified by Folate-PEG-Lipid for Targeted Drug Delivery to Cancer Cells *In Vitro*

Akihiro Hayama[1], Tatsuhiro Yamamoto[2], Masayuki Yokoyama[2], Kumi Kawano[1], Yoshiyuki Hattori[1], and Yoshie Maitani[1,*]

[1] *Institute of Medicinal Chemistry, Hoshi University, 2-4-41 Ebara, Shinagawa-ku, Tokyo 142-8501, Japan*
[2] *Kanagawa Academy of Science and Technology, KSP East 404, Sakado 3-2-1, Takatsu-ku, Kawasaki-shi, Kanagawa 213-0012, Japan*

A novel technique was developed for the formation of ligand-targeted polymeric micelles that can be applicable to various ligands. For tumor-specific drug delivery, camptothecin (CPT)-loaded polymeric micelles were modified by folate to produce a folate-receptor-targeted drug carrier. Folate-linked PEG_{5000}-distearoylphosphatidylethanolamine (folate-PEG_{5000}-DSPE) was added when preparations of drug-loaded polymeric micelles, resulting in folate ligands exposed to the surface. Folate-modified CPT-loaded polymeric micelles (F-micelle) were evaluated by measuring cellular uptake using a flow cytometer, fluorescence microscopy, and confocal laser scanning microscopy, and by cytotoxicity measurement. The results revealed that F-micelle showed higher cellular uptake in KB cells over-expressing folate receptor (FR) and higher cytotoxicity compared with non-folate modified CPT-loaded polymeric micelles (plain micelles) in KB cells, but not in FR-negative HepG2 cells. This result indicated that polymeric micelles were successfully modified by the folate-linked lipid.

Keywords: Polymeric Micelles, Camptothecin, Targeting, Folate-PEG-Lipid, Folate.

RESEARCH ARTICLE

1. INTRODUCTION

Camptothecin (CPT) has shown a broad spectrum of antitumor activity;[1,2] however, its clinical use of CPT has some drawbacks, mainly due to water insolubility and aqueous instability of the lactone ring moiety. The lactone ring opens rapidly at physiological pH or above, resulting in a complete loss of biological activity.[3,4]

Nanoparticles including polymeric micelles have attracted much attention in drug delivery research. Polymeric micelles are prepared from block copolymers possessing both hydrophilic and hydrophobic chains.[5,6] Their advantageous characteristics for drug targeting include solubilization of hydrophobic molecules and high structural stability. CPT-loaded polymeric micelles enhanced the anticancer activity of CPT against solid tumors because of their prolonged blood circulation and higher accumulation in tumors.[7,8]

As with other carriers, ligand-mediated targeting of polymeric micelles to target receptors expressed selectively or over-expressed on tumor cells is increasingly recognized as an effective strategy for improving the therapeutic effect of anticancer drugs. If CPT can facilitate tumor targeting, a great contribution to the cancer chemotherapy is feasible. A variety of targeting ligands has been examined as tumor-targeted drug carriers. Folate receptor (FR) is abundantly expressed in a large percentage of human tumors, but it is only minimally distributed in normal tissue;[9] therefore, FR can serve as a functional tumor-specific receptor. Folate modification of polymeric micelles has been reported to covalently conjugate block copolymer with folate.[10,11] In these methods, the type of ligand must be decided in the preparation of polymeric micelles. In other words, the ligand-polymer conjugate must be synthesized with conformity to the drug. It is already known that a proper amount of folate-PEG-lipids could be inserted in liposomes and emulsions without change of their stability, and folate lipid-modified liposomes and emulsions with longer polyethylene glycol (PEG) linker were taken effectively by the FR-mediated cellular uptake.[12,13] However, it has been no reports about surface-modified polymeric micelles by lipid. In polymer micelles, folate might not be able to be exposed outside by steric configuration of the hydrophilic block chain. Properties of the inner core such as hydrophobicity and rigidity, were very important to achieve micelles with stable drug incorporation.[7,8,14] Folate lipid modification, therefore might affect the properties of the inner cores.

*Author to whom correspondence should be addressed.

1533-4880/2007/8/001/006 doi:10.1166/jnn.2007.093

For targeted drug delivery to cancer cells, we prepared folate-modified CPT-loaded polymeric micelles (F-micelle), and evaluated by measuring cellular uptake using a flow cytometer, fluorescence microscopy, and confocal laser scanning microscopy, and by cytotoxicity measurement. In this paper, we describe a novel method of folate modification to CPT-loaded polymeric micelles by folate-linked PEG_{5000}-distearoylphosphatidylethanolamine (folate-PEG_{5000}-DSPE).

2. MATERIALS AND METHODS

2.1. Materials

Poly(ethylene glycol)-poly(benzyl aspartate-53) block copolymer (PEG-P(Asp(Bz53))) was synthesized as described previously.[14,15] The molecular weight of the PEG block was 2000 and the average number of aspartate units was 17. Fifty-three percentage of the aspartic acid residue was esterified with the benzyl group. CPT and folic acid were purchased from Wako Pure Chemicals (Tokyo, Japan). Folate-PEG_{5000}-DSPE was synthesized as described previously.[12,13] 1,1′-Dioctadecyl-3,3,3′,3′-tetramethylindocarbocyanine perchlorate (DiI) was purchased from Lambda Probes and Diagnostics (Graz, Austria).

2.2. Preparation of Folate-Modified CPT-Loaded Polymeric Micelles (F-Micelles)

CPT was incorporated into polymeric micelles by an evaporation method as described previously,[15] using 0.5 mg of CPT, 5 mg of block copolymer, and 0 mol%, 0.03 mol% (0.027 mg), 0.1 mol% (0.092 mg) and 0.2 mol% (0.18 mg) of folate-PEG_{5000}-DSPE to CPT loaded in micelles for plain micelles, 0.03F-micelle, 0.1F-micelle and 0.2F-micelle, respectively. DiI-labeled F-micelles were prepared by the same protocol, but with the post-addition of DiI at 0.4 mol% of incorporated CPT. The incorporation efficiency was calculated as described previously.[15] The mean particle diameters and ζ-potentials were determined using a particle size analyzer (ELS-Z, Otsuka Electronics, Osaka, Japan) at 25 °C by diluting the dispersion to an appropriate volume with water.

2.3. *In Vitro* Drug Release

Release of CPT in F-micelles from a dialysis tube was measured using seamless cellulose tube membranes (Viskase Sales Corp., IL, USA) with a molecular cut-off of 12,000–14,000. The initial concentration of CPT was 10 μg/ml. The sample volume in the dialysis bag was 1 ml and the sink volume was 200 ml PBS at pH 7.4 with the medium at 37 ± 0.1 °C. The drug concentration was analyzed using fluorescence spectrophotometer F-4010 (Hitachi, Tokyo, Japan) (excitation 369 nm, emission 426 nm).

2.4. Cell Culture

KB cells (FR (+)) and HepG2 cells (FR (−)) were obtained from the Cell Resource Center for Biomedical Research, Tohoku University (Miyagi, Japan). Both cells were cultured in folate-deficient RPMI 1640 medium (Invitrogen Corp., Carlsbad, CA, USA) with 10% heat-inactivated fetal bovine serum (Invitrogen Corp.) and 100 μg/ml kanamycin with 5% CO_2 at 37 ° C.

2.5. Flow Cytometry Analysis

KB cells were prepared by plating 5×10^5 cells in a 6-well culture plate 1 day before the assay. Cells were incubated with DiI-labeled F-micelles containing 10 μg CPT/ml diluted in 2 ml folate-deficient RPMI 1640 medium for 2 hours at 37 °C. In free-folic acid competition studies, 2 mM folic acid was added to the medium. After incubation, cells were washed two times with acidic saline (pH 3) followed by one wash with cold phosphate-buffered saline (PBS, pH 7.4) to remove unbound polymeric micelles, detached with 0.02% EDTA-PBS, and then suspended in PBS containing 0.1% bovine serum albumin and 1 mM EDTA. The suspended cells were directly introduced to a FACSCalibur flow cytometer (Becton Dickinson, San Jose, CA, USA) equipped with a 488 nm argon ion laser. Data for 10,000 fluorescent events were obtained by recording forward scatter, side scatter, and 585/42 nm fluorescence. The autofluorescence of cells was taken as a control.

2.6. Fluorescence and Confocal Laser Scanning Microscopy

After incubation, cells were washed as described above; 2 ml fresh medium was added. The cells were observed with fluorescence microscopy (ECLIPSE TS100, Nikon, Tokyo, Japan) at just. For confocal laser scanning microscopy, cells were fixed with Mildform 20 N for 30 min at room temperature. Subsequently, the cells were washed three times with PBS. Examinations were performed with a Radiance 2100 confocal laser-scanning microscope (BioRad, CA, USA).

2.7. Cytotoxicity Study

Cells were prepared by plating 1×10^4 cells in a 96-well culture plate 1 day before the experiment. KB and HepG2 cells were then incubated for 2 hours at 37 °C with 100 μl CPT solution, plain micelle, and F-micelles (containing 0.01, 0.1, 0.5, 1, 2.5 and 5 μg CPT) diluted in folate-deficient RPMI 1640 medium. The medium was replaced with fresh medium and incubated for a further 48 hours. Cytotoxicity was determined with the WST-8 assay (Dojindo Laboratories, Kumamoto, Japan). The number of viable cells was then determined by absorbance measured at 450 nm on an automated plate reader (BioRad, CA, USA).

2.8. Statistical Analysis

Statistical comparisons were performed by Student's t-test. P values less than 0.05 were considered significant.

3. RESULTS AND DISCUSSION

3.1. Determination of CPT Content and Particle Size of F-Micelles

In our previous study, folate modification with a sufficiently long PEG chain on emulsion is an effective way of targeting drug carriers to tumor cells.[13] Therefore, folate-lipid conjugate with PEG_{5000} linker was used for the modification of polymeric micelles with PEG_{2000}. Four kinds of CPT-loaded polymeric micelles were formulated as plain micelles, 0.03F-micelle, 0.1F-micelle and 0.2F-micelle. Folate-PEG-DSPE may be incorporated to polymeric micelles since 0.2 mol% folate-PEG_{5000}-DSPE was 9.6 μM, and the critical micelle concentration (CMC) value of folate-PEG_{5000}-DSPE was 12.1 μM determined by the fluorescence probe technique using DiI.

The average particle size of each F-micelle in water was about 230 nm with 0.5–1.1 mV in ζ-potential and the CPT-loading efficiency was about 50%. These values of F-micelles did not change significantly compared with plain micelles.

3.2. *In Vitro* Drug Release

The *in vitro* release of CPT from 0.03F-micelle exhibited rapid release behavior in an early stage (about 40% in 2 hours, Fig. 1). In contrast, the release of CPT from 0.2F-micelle and plain micelles reached only about 20% after the same period of incubation. This result indicates that the quantity of folate modification affected the stability of polymeric micelles, indicating that the higher the folate surface density, the lower the drug release. Similar results were reported that folate modification of liposomes influenced the release pattern.[16] The decreased drug release from highly folate-modified polymer micelles might be due to the structural integrity of folate coupling, that may lead to barrier effect for CPT diffusion.

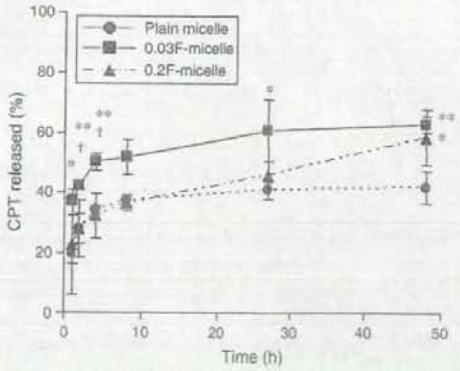

Fig. 1. Release profiles from plain and folate-modified CPT-loaded polymeric micelles at 37 °C in PBS as a sink solution at pH = 7.4. Each value represents the mean ± S.D. ($n = 3$). $^{*}P < 0.05$, $^{**}P < 0.01$ compared with plain micelle, $^{\dagger}P < 0.05$ compared with 0.2F-micelle.

3.3. Uptake of F-Micelles to KB Cells

Cellular uptake of F-micelle was evaluated using polymeric micelles labeled with DiI by flow cytometry. The fluorescence of 10 μg CPT/ml of DiI-labeled plain

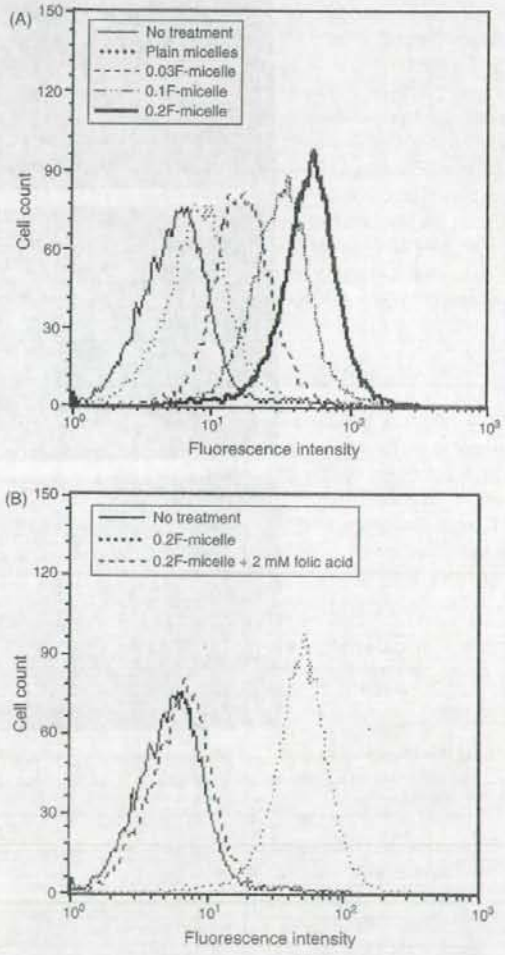

Fig. 2. Uptake of DiI-labeled plain and folate-modified CPT-loaded polymeric micelles with KB cells in the absence (A), or presence of 2 mM folic acid (B). Cells were incubated with polymeric micelles in folate-free RPMI 1640 medium for 2 hours at 37 °C and analyzed by flow cytometry. No treatment indicates autofluorescence of untreated cells. Each analysis was generated by counting 10^4 cells.

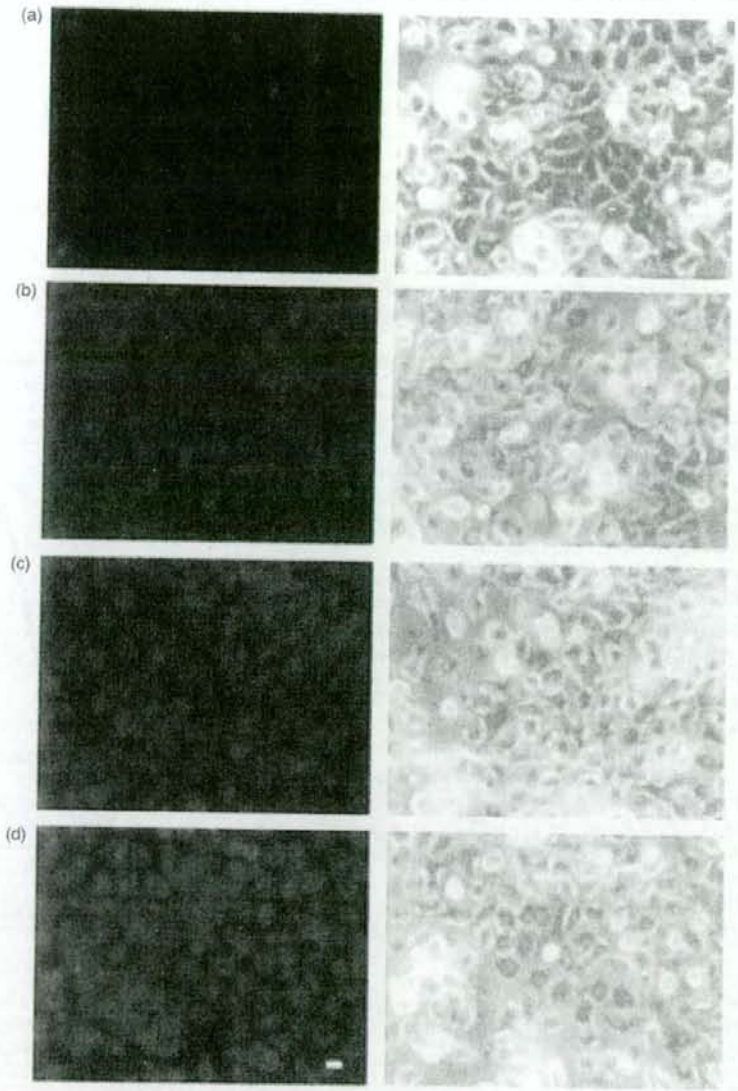

Fig. 3. Fluorescence microscopic images of KB cells treated with (a) plain micelles, (b) 0.03F-micelle, (c) 0.1F-micelle and (d) 0.2F-micelle. Cells were incubated with polymeric micelles in folate-free RPMI 1640 medium for 2 hours at 37 °C, then observed just after. (×200) Scale bar denotes 10 μm.

micelles and F-micelles showed almost identical spectrofluorimetric units (data not shown). As shown in Figure 2(A), flow cytometry analysis represented a shift in the curve. 0.2F-micelle indicated higher mean intensity of about 13.8-fold, 7.9-fold and 3.3-fold in cellular association of plain micelles, 0.03F-micelle and 0.1F-micelle after 2 hours exposure, respectively. In contrast, micelles modified with methoxy-PEG$_{5000}$-DSPE showed a similar curve to plain micelles (data not shown). Additionally, these increased associations of 0.03F-micelle, 0.1F-micelle (data not shown) and 0.2F-micelle could be completely blocked by adding 2 mM folic acid to the medium (Fig. 2(B)). This is the first report showing that folate-lipid was incorporated and its folate group was exposed on the surface of polymeric micelles to interact with FR. The results also indicate that F-micelle was transported within cells by an FR-mediated endocytosis process. These findings are consistent with those reported previously on the FR-mediated cellular uptake of folate-modified liposomes and emulsions for anti-cancer therapy.[12, 13]

Cellular uptake of F-micelles was also evaluated using fluorescence microscopy. Fluorescence images of KB cells after incubation with F-micelles for 2 hours are shown in Figure 3. For plain micelles, there was no remarkable uptake in fluorescent intensity of KB cells. In contrast, in F-micelles, more fluorescently labeled cells could be clearly visualized, and 0.2F-micelle was especially taken up in to the cells. This result is similar to that of flow cytometry. In accordance with the results from flow cytometry analysis, fluorescence microscopy confirmed that F-micelles could be targeted to cancer cells over-expressing FR on their surface.

3.4. Localization of F-Micelles to KB Cells

To investigate whether F-micelles existed on cell surface or within cells, localization of F-micelles was evaluated using confocal laser scanning microscopy. Fluorescence images of KB cells after incubation with 0.03F-micelle for 2 hours are shown in Figure 4. 0.2F-micelle showed similar image (data not shown). The localization of DiI-labeled F-micelles was confirmed by changing the Z-axis of observed area with 1 μm. DiI-fluorescence was detected as punctuate dots within cells. This indicated that F-micelles were internalized into the cells and located within endosome compartments.

3.5. Cytotoxicity Study

FR-targeted polymeric micelles were evaluated for *in vitro* cytotoxicity in FR (+) KB and FR (−) HepG2 cells by WST-8 assay. Superior cytotoxicity of F-micelles over plain micelles was observed in KB cells, but not in HepG2 cells. IC_{50} values for KB cells of F-micelles were about 2–3 times lower than the plain micelles (Table I). The difference of IC_{50} values between 0.03F-micelle and 0.2F-micelle was not large. It might be due to the release of CPT from 0.03F-micelle was faster than that from 0.2F-micelle, and free CPT was taken up to the cells as well as micelles. In contrast, IC_{50} values for HepG2 cells show hardly any difference between F-micelles and plain micelles.

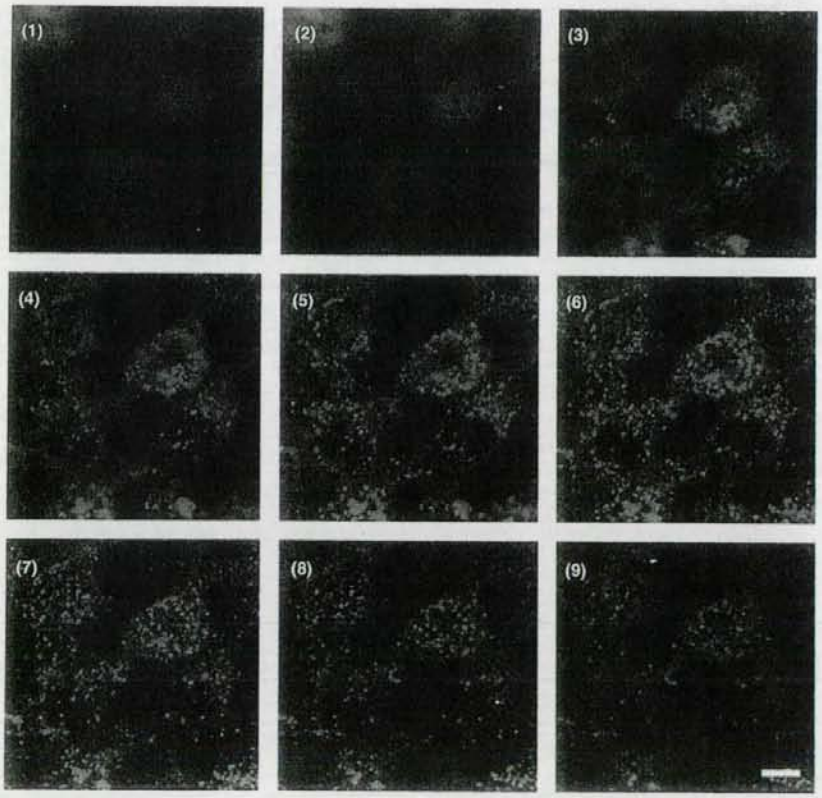

Fig. 4. Localization of DiI-labeled folate-modified CPT-loaded polymeric micelles (0.03F-micelle) with KB cells. Cells were incubated with polymeric micelles in folate-free RPMI 1640 medium for 2 hours at 37 °C, then observed just after under confocal laser scanning microscopy by changing the Z-axis. Images (1–9) represent regular intervals of 1 μm on the Z-axis from bottom to top cells, respectively. (×1200) Scale bars denote 10 μm.